ELSEVIER

Earth and Planetary Science Letters 134 (1995) 23–36

EPSL

Production of Jurassic rhyolite by anatexis of the lower crust of Patagonia

R.J. Pankhurst [a,*], C.R. Rapela [b]

[a] *British Antarctic Survey, c/o NERC Isotope Geosciences Laboratory, Kingsley Dunham Centre, Keyworth, Nottingham NG12 5GG, UK*
[b] *Centro de Investigaciones Geológicas, CONICET–Universidad Nacional de La Plata, 644 Calle No. 1, 1900 La Plata, Argentina*

Received 29 September 1994; accepted 24 May 1995

Abstract

The mid-Jurassic Marifil and Chon-Aike volcanic rocks of eastern Patagonia are part of one of the largest silicic igneous provinces known. Rb–Sr geochronology indicates eruptive ages of 175–190 Ma for the Marifil complex (mostly Toarcian–Aalenian). The majority of the rocks are isotopically uniform, with initial $^{87}Sr/^{86}Sr = 0.7067 \pm 0.0003$ and $\epsilon Nd_t = -4 \pm 2$. Primary magmas of andesitic composition were generated by partial melting of mafic "Grenvillian" lower crust, indentified by depleted-mantle model ages of 1150–1600 Ma. Lower crustal pyroxene–granulite xenoliths can be modelled as residual Jurassic source, although they may alternatively be co-genetic cumulates. The dacite–rhyolite suite formed by crystal–liquid fractionation processes from the primary andesites: involving multistage crystallization and re-melting during magma ascent, with the later stages of evolution being explicable by fractional crystallization of plagioclase, amphibole and accessory minerals. The province represents large-scale lower crustal reworking associated with the unique tectonic and igneous environment of Gondwana break-up.

1. Introduction

The origin of large-scale silicic igneous provinces remains a controversial topic in igneous petrology. The Tertiary rhyolites and ignimbrites of the Sierra Madre Occidental, Mexico have been ascribed to differentiation of mantle-derived magmas [1,2], or lower crustal anatexis [3]—(see also discussion in *Contributions to Mineralogy and Petrology* 104, 609–618, 1990). Much of the debate concerns the interpretation of geochemical and isotope data for the volcanic rocks and for local xenolithic material that may represent lower crustal compositions. We report similar data for silicic volcanic rocks in southern South America that constitute a province as large as, if not larger than, the Sierra Madre Occidental. These, in our view, tend to support the lower crustal anatexis model. Crystal–liquid fractionation is responsible for the diversity observed, but remelting of basaltic andesite in the lower crust is as important as fractional crystallization.

2. Geological setting

The Mesozoic acid volcanic province of Patagonia [4] covers an area of about 1 million km^2, and in many places it has a demonstrable minimum thickness of 500 m. Its separate centres or outcrop areas

* Corresponding author

SSDI 0012-821X(95)00103-4

(Fig. 1) are associated with local formation names (e.g. Marifil, Chon-Aike, El Quemado, Ibañez, Tobífera). If Late Palaeozoic volcanic rocks in central Argentina, which extend into northern Patagonia, and Jurassic igneous rocks in West Antarctica are also considered as genetically related [5], then the province is enormous.

Rhyolite occurs throughout the province, and predominates in the northeast, where the Marifil complex largely consists of welded crystal ignimbrite units and sub-horizontal massive ash/lava flows, each up to 100 m thick, with subordinate lithic ignimbrites. In the southeast, the Chon-Aike Formation also consists mostly of rhyolite–trachydacite

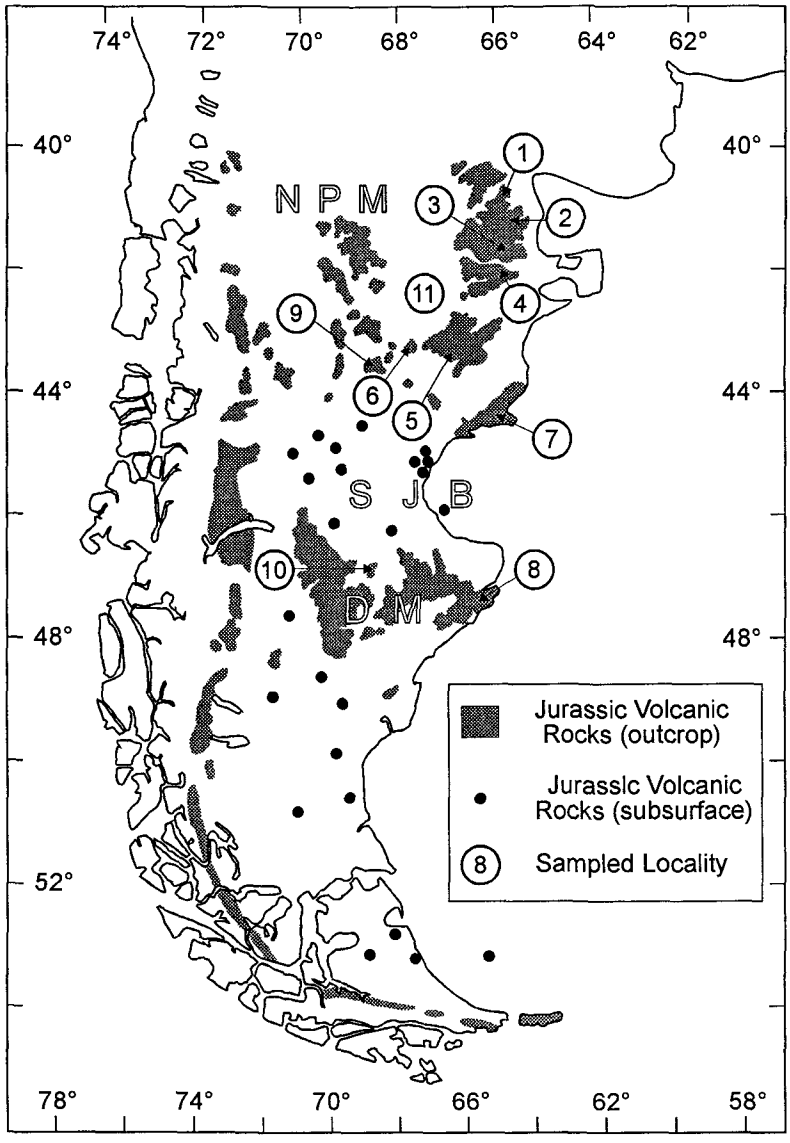

Fig. 1. The Jurassic volcanic province of Patagonia [4]. Sampled localities: *1* = Sierra Pailemán, *2* = Sierra Grande, *3* = Estancia Marifil, *4* = Sierra Negra, *5* = Dique Ameghino, *6* = Río Chubut, *7* = Península Camarones, *8* = Puerto Deseado, *9* = Los Altares (Lonco Trapial Formation), *10* = Bajo Pobre, *11* = Sierra de Los Chacays. *NPM* = North Patagonian Massif; *DM* = Deseado Massif; *SJB* = San Jorge Basin.

pyroclastic rocks and flows, and subvolcanic rhyolite domes. In the Río Chubut section, the rhyolites interdigitate with the andesitic Lonco–Trapial Formation, which occupies much of north-central Patagonia. In the Andean Cordillera, both rhyolite and andesite are involved, but folding has produced a more broken outcrop pattern (El Quemado, Ibañez and Tobífera formations) and hydrothermal alteration/low-grade metamorphism also increases due to Andean deformation and burial beneath the Cretaceous sediments of the Magellanes basin. The present work concentrates on the geochronology, geochemistry and isotope geology of the eastern rhyolitic outcrops: the Marifil and Chon-Aike complexes (the latter in only a preliminary manner), and is an extension of our previous work [6], which also gives geological references. We have also analysed samples of the possibly contemporaneous andesites of the Bajo Pobre Formation of the Deseado Massif and lower crustal xenoliths in a Tertiary ultrapotassic latite plug in the Sierra de Los Chacays [7] that we believe are significant in the history of the rhyolite genesis.

3. Analytical methods

Rb–Sr whole-rock analyses were carried out at the NERC Isotope Geosciences Laboratory, Keyworth. Rb/Sr ratios were determined by X-ray fluorescence; precision is $\pm 0.5\%$ (1σ) for concentrations > 50 ppm, and this level of long-term consistency has been proven to apply to ages calculated from favourable Rb/Sr spreads by repeatedly reanalysing "in-house" isochron sets. Sr isotope compositions were determined on a Finnegan-MAT 262 mass-spectrometer with static multichannel collection, to an internal precision of better than 10 ppm (1 s.e.m.). During the earlier stage of the study [6], the NBS987 standard gave a mean $^{87}Sr/^{86}Sr$ ratio of 0.710240. For the present analyses this had dropped to 0.710190 ± 0.000009 (1σ): measured ratios were therefore corrected to be consistent with the previous data, by direct proportion, and corrected results are presented in Table 1. For isochron calculations, the overall reproducibility of $^{87}Sr/^{86}Sr$ ratios is considered to be 0.01% (1σ) for normal compositions (up to 0.03% at values > 1). All errors on ages are quoted as $\pm 2\sigma$.

Table 1
New Rb–Sr data

Sample	Type*	Rb ppm	Sr ppm	$^{87}Rb/^{86}Sr$	$^{87}Sr/^{86}Sr$
Marifil complex: Sierra Paileman (188 Ma)					
PAI-02	HSR	516	33	46.183	0.830285
PAI-03	HSR	510	44	33.572	0.797492
PAI-04		365	25	42.957	0.819544
PAI-05	HSR	381	27	41.698	0.815274
PAI-06	A	82	1012	0.233	0.707765
PAI-07	D	104	948	0.318	0.707975
PAI-08		457	37	36.526	0.803819
PAI-09		357	27	39.225	0.812920
PAI-12		289	164	5.085	0.720956
PAI-10	HSR	552	86	18.661	0.762517
PAI-11	HSR	523	67	22.552	0.773390
Marifil complex: Sierra Grande (174 Ma)					
SG-01		586	120	14.170	0.747571
SG-02	HSR	587	111	15.402	0.750797
SG-05		760	17	130.327	1.038940
SG-06	HSR	512	37	40.036	0.811285
SG-07		411	48	24.810	0.773939
SG-08		555	107	15.060	0.750205
SG-09	HSR	557	23	70.091	0.886487
SG-11		538	96	16.216	0.752649
SG-12		536	84	18.464	0.758272
SG-13	HSR	549	99	16.160	0.752701
SG-04		197	181	3.156	0.715466
SG-10	LSR	487	89	15.923	0.748492
SG-14	HSR	622	20	92.652	0.943333
Marifil complex: Rio Chubut (169 Ma)					
Taque-12	D	127	443	0.831	0.708550
Taque-13	A	71	680	0.303	0.707257
Taque-14		102	519	0.568	0.708102
Taque-15	HSR	109	263	1.193	0.709591
Taque-16	LSR	108	392	0.797	0.708620
Taque-17		126	293	1.243	0.709521
Taque-18	LSR	117	363	0.933	0.708370
Taque-19	HSR	191	26	21.604	0.757643
Taque-21	HSR	179	28	18.306	0.751472
Taque-22		183	21	25.858	0.767326
Bajo Pobre andesites (?175 Ma)					
BP3	BA	46	457	0.290	0.707707
BP5	A	43	297	0.421	0.707722
BP7	A	55	365	0.432	0.707350
BP9	A	63	386	0.474	0.707891
BP10	A	66	408	0.469	0.706618
BP11	A	66	598	0.319	0.706354
Sierra de Los Chacays xenoliths					
NCHAC-1		1	518	0.006	0.706784
NCHAC-2		2	682	0.008	0.706692
NCHAC-3		1	555	0.004	0.707820
NCHAC-4		1	46	0.037	0.706639
NCHAC-5		1	16	0.155	0.706225
NCHAC-7		1	744	0.003	0.706509
NCHAC-R		137	1001	0.396	0.706397
Standards (No of determinations)					
NBS70a (2)		527	65	24.474	1.20157
JG-1 (3)					0.711004
JB-1 (7)					0.704105
BHVO-1 (4)					0.703468

Analytical methods as in Rapela and Pankhurst [6], except that results are adjusted from determined mean value of 0.710190 ± 0.000009 for NBS987, to the previously obtained 0.710235.

* Rock type—see Fig. 3

Sm–Nd analyses were performed by isotope dilution with a mixed ^{149}Sm–^{150}Nd spike, using HDEHP-coated polystyrene columns for the REE separation. Measurements were carried out on a fully automated VG 354 mass-spectrometer, using static collection to determine the Sm and Nd concentrations, and mixed static/peak-jumping to determine the $^{143}Nd/^{144}Nd$ ratios with an internal precision of ± 10 ppm (1 s.e.m.). Long-term reproducibility of $^{143}Nd/^{144}Nd$ ratios both on the La Jolla and in-house standards is better than 15 ppm (1σ), but on rock standards this rises to 30–40 ppm. Sm/Nd ratios on rock standards are reproducible to 0.1–0.2% (1σ). Data are presented in Table 2.

Most geochemical analyses were carried out in the Centro de Investigaciones Geológicas, La Plata. Al, total Fe, Ca, Mg, Mn, Na and K were determined by AAS; Si, P and Ti by colorimetry and Fe^{2+} by volumetry; Y, Zr and Nb by X-ray fluorescence [8] and REE by ICP-AES. Reproducibility for the REE contents of the standard granite AC–E shown in Table 3 varies 3–5% (1σ). REE in critical samples were re-analysed at Royal Holloway and Bedford New College, London University, also using ICP-AES, but for a fuller range of elements. Representative analyses are presented in Table 3; in total about 80 samples were analysed for major elements and almost half of these for trace elements and REE.

4. Geochronology and isotope characteristics

Stratigraphic constraints on the acid volcanism are post-Middle/Upper Triassic for the Marifil complex

Table 2
Sm–Nd data for Jurassic volcanic rocks of Patagonia and crustal nodules

Sample	Locality	Type	Age Ma	Sm ppm	Nd ppm	$^{147}Sm/^{144}Nd$	$^{143}Nd/^{144}Nd$	εNd_t	T_{DM}
PAI-2	1	HSR	188	8.316	39.368	0.1277	0.512256	-5.8	1454
PAI-7	1	D	188	7.811	46.157	0.1023	0.512210	-6.1	1475
SG-6	2	HSR	174	4.909	29.057	0.1021	0.512326	-4.0	1310
SG-7	2		174	4.759	26.586	0.1082	0.512300	-4.7	1358
SG-10	2	LSR	174	9.538	53.006	0.1088	0.512327	-4.2	1319
SG-11	2		174	3.663	21.566	0.1027	0.512330	-4.0	1305
CON89-42	4	LSR	183	7.417	43.809	0.1024	0.512148	-7.4	1556
CON89-44B	4	TD	183	8.584	50.493	0.1028	0.512122	-7.9	1600
CON89-37B	4		183	7.231	42.116	0.1038	0.512197	-6.5	1457
DA7	5	BA	181	7.668	41.510	0.1117	0.512339	-3.9	1305
DA2	5	HSR	181	5.237	32.657	0.0969	0.512292	-4.5	1349
DA10	5	HSR	181	4.634	24.204	0.1157	0.512330	-4.2	1326
TAQUE-13	6	A	169	6.156	32.633	0.1140	0.512241	-6.0	1454
MELO-9	6	HSR	169	15.931	88.528	0.1088	0.512324	-4.2	1323
MELO-11	7	LSR	178	14.374	81.343	0.1068	0.512306	-4.5	1346
BL IIe	8		168	24.860	117.643	0.1292	0.512472	-1.8	1135
PD130	8	HSR	168	5.095	28.132	0.1095	0.512419	-2.4	1182
PD128	8	TD	168	7.422	38.646	0.1161	0.512352	-3.9	1295
BP3	10	BA	175	10.767	51.909	0.1254	0.512362	-3.8	1295
BP5	10	A	175	3.188	15.027	0.1282	0.512340	-4.3	1333
BP7	10	A	175	3.172	14.867	0.1290	0.512347	-4.2	1324
BP9	10	A	175	3.075	14.469	0.1285	0.512351	-4.1	1317
NCHAC-1	11		180	1.284	4.747	0.1635	0.512424	-3.5	1270
NCHAC-2	11		180	1.213	4.764	0.1539	0.512393	-3.8	1299
NCHAC-3	11		180	1.602	4.994	0.1939	0.512289	-6.8	1537
NCHAC-4	11		180	0.939	1.697	0.3344	0.512578	-4.4	1340
NCHAC-5	11		180	0.261	0.911	0.1730	0.512500	-2.2	1187
NCHAC-7	11		180	0.574	1.864	0.1863	0.512473	-3.0	1236
NCHAC-R	11		30	12.134	74.165	0.0989	0.512456	-3.2	1149
BHVO-1 (5)	Standard			6.121	24.601	0.1504	0.512984	+6.7	

Mean value of Johnson–Matthey Nd = 0.511122 ± 0.000016 (1σ), corresponding to 0.511858 for La Jolla. Rock Types as in Fig. 3. T_{DM} is depleted mantle model age (Ma) after DePaolo et al. [31].

and post-Early Jurassic for the Chon-Aike complex. In the Río Chubut section, volcanic rocks of the Marifil and Lonco-Trapial complexes are overlain by lowermost Cretaceous. It is usually considered that volcanism started in Late Triassic times and reached a climax in Middle Jurasssic (Pliensbachian–Bajocian), but activity may have continued into Late Jurassic times in the Andean outcrops(see [4] for references). Published K–Ar ages range from mid-Triassic to Cretaceous, with an peak in the interval 155–165 Ma; although this was considered by Cortés [9] to be consistent with the stratigraphic evidence, according to more recent time scales this range is entirely post-Bajocian.

Rb–Sr whole-rock isochron dating [6] has shown that at four of its main outcrops (localities 3, 4, 5 and 7 in Fig. 1), the Marifil complex was extruded during a brief period from 183 ± 2 to 178 ± 1 Ma (Toarcian–Aalenian). New data for the three remaining outcrops of the Marifil complex are plotted in Fig. 2. These show more scatter than in the earlier work, perhaps due to secondary effects: exclusion of the few clearly aberrant points results in isochron ages of 188 ± 1 Ma (Pliensbachian), 174 ± 2 Ma (Aalenian) and 169 ± 2 Ma (Bajocian) respectively. At Sierra Grande, the high initial $^{87}Sr/^{86}Sr$ ratio for the majority of the samples (0.7127 ± 0.0006) is distinctive and may well signify rotation of the isochron during post-eruptive re-homogenization (large K-feldspar phenocrysts in the rhyolites show patchy and vein replacement by another, probably secondary, K-feldspar). The Chon-Aike volcanism of

Table 3
Representative whole-rock geochemical analyses

Sample	PAI -2	PAI -6	SG -10	CON89 -42	DA -10	DA -7	TAQUE -13	MELO -9	PD -128	BP -9	BP -5	CHAC -2	CHAC -3	CHAC -7	AC-E
Type	HSR	A	LSR	LSR	HSR	BA	BA	HSR	TD	A	A				
Locality	1	1	2	4	5	5	6	7	8	10	10	11	11	11	(Std)
SiO2	77.20	61.56	73.64	71.81	77.67	52.32	62.61	75.81	67.47	58.71	59.51	46.03	45.16	51.44	
TiO2	0.29	1.00	0.40	0.37	0.08	0.95	0.79	0.42	0.40	0.64	0.67	0.23	1.73	0.20	
Al2O3	12.11	15.25	13.89	14.10	13.66	19.73	15.21	11.87	16.81	18.10	17.78	18.12	18.11	19.25	
Fe2O3	0.51	5.10	2.20	1.85	0.91	3.53	1.96	1.74	4.98	2.10	2.28	3.56	6.08	0.79	
FeO	0.19	0.71	0.16	0.65	0.16	5.76	3.82	0.01		4.70	4.42	3.99	7.34	3.71	
MnO	0.01	0.15	0.13	0.07	0.10	0.13	0.01	0.08	0.05	0.10	0.09	0.12	0.16	0.09	
MgO	0.10	2.21	0.50	0.69	0.26	3.64	3.80	0.06	0.20	4.72	4.63	16.70	8.95	14.68	
CaO	0.04	7.29	1.04	2.15	0.18	8.81	6.63	0.17	1.46	7.48	7.11	10.24	11.44	8.30	
Na2O	0.29	3.05	1.25	3.39	2.00	2.32	2.84	3.79	4.80	1.47	1.69	0.71	0.73	1.37	
K2O	9.08	3.12	6.56	4.85	4.63	2.19	1.93	6.01	3.56	1.75	1.59	0.13	0.11	0.10	
P2O5	0.17	0.56	0.22	0.09	0.33	0.61	0.41	0.04	0.27	0.22	0.24	0.15	0.17	0.07	
Rb	516	82	487	163	181	51	71	208	77	63	43	2	1	1	
Sr	33	1012	89	280	23	422	680	28	445	386	297	682	555	744	
Y	37	19	39	22	17	25	16	47		19	13	5	9.7	7.4	
Nb	19	10	32	13	10	5	3	26		2	2	0			
Zr	146	338	256	268	110	278	268	544		119	106	140	92	156	
La	40.7	45.3	66.8	67.2	30	38.7	28.7	90.6	39.59	14.5	14.2	2.7	2.3	1.4	59.3
Ce	88.5	96.1	141.2	124.3	65.1	83.0	63.2	188.3	86.0	32.0	31.3	7.1	5.9	2.6	155.2
Pr	10.4	10.93	15.18		6.63	10.02	7.57			3.66	3.62	1.05	0.92	0.39	
Nd	36.6	40.8	50.3	45.4	21.4	38.4	27.7	88.8	39.53	14	14.1	4.8	5.3	2.1	92.1
Sm	7.75	6.9	8.8	8.7	4.34	6.88	5.26	17.86	8.08	3.08	3	1.15	1.52	0.6	22.2
Eu	0.44	1.79	1.22	0.9	0.42	1.78	1.27	1.25	1.8	0.77	0.78	0.45	0.59	0.29	1.7
Gd	6.31	5.56	7.02	6.7	3.52	5.78	4.4	12.08		2.84	2.71	1.14	1.77	0.66	24.1
Tb									0.99						
Dy	5.59	3.86	6.52	5.7	3.5	4.33	3.05			2.5	2.26	0.88	1.63	0.57	29.6
Ho	1.15	0.81	1.38		0.76	0.89	0.63			0.53	0.48	0.18	0.34	0.11	5.3
Er	3.13	2.06	4	3	2.24	2.36	1.66	5.39		1.5	1.36	0.5	0.96	0.38	17.4
Yb	3.06	1.93	4.09	2.8	2.53	2.1	1.52	4.95	2.63	1.52	1.33	0.41	0.8	0.32	16.8
Lu	0.45	0.3	0.62	0.4	0.4	0.32	0.23	0.77	0.37	0.24	0.22	0.07	0.12	0.05	2.3

Major element concentrations are recalculated to 100% on a water-free basis. Major and Rare Earth Elements determined by ICP spectrometry in La Plata or RHBNC, except for PD-128 which was analysed by INAA at Cornell University by P. Sruoga and has been previously published [10]; Rb, Sr from Table 2; Y, Nb, Zr by XRF spectrometry in La Plata. Rock types as in Fig. 3.

the Deseado Massif, still farther to the south, has yielded a preliminary Rb–Sr age of 168 ± 2 Ma [10], corresponding to Bajocian. All the Rb–Sr results are concordant with local stratigraphic controls and imply that eruption occurred during a relatively short interval locally, but with significant southward diachronism of activity, over as much as 20 Ma.

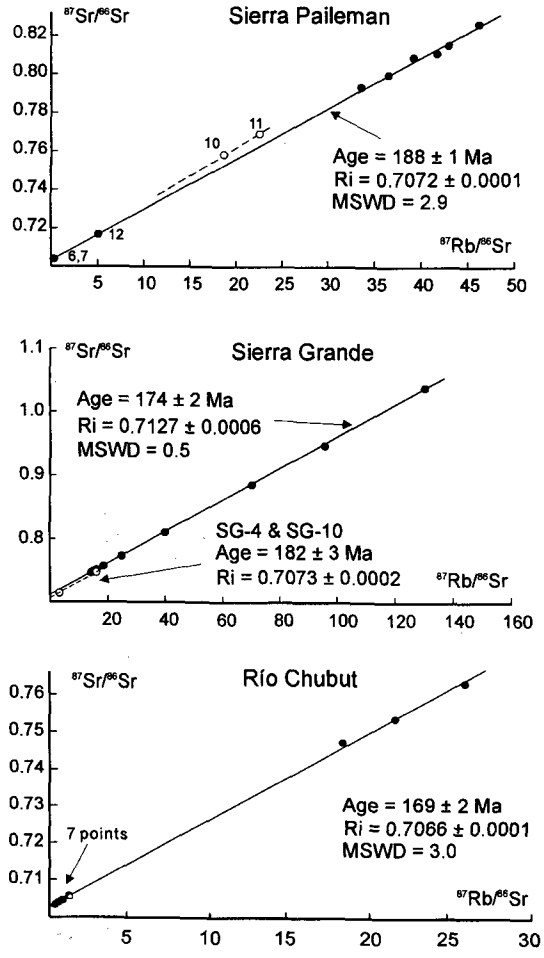

Fig. 2. Rb–Sr isochrons for localities 1, 2 and 6 (Fig. 1). Unshaded points are excluded: (a) PAI-10 and -11, from a small rhyolite dome, may be genuinely older, or contaminated with basement Sr. (b) The main suite has an unusually high initial $^{87}Sr/^{86}Sr$ ratio of 0.7127, but two samples give a slightly older age and the "normal" initial $^{87}Sr/^{86}Sr$ ratio of 0.707. The main suite may have been re-homogenized during post-crystallization hydrothemal activity. (c) There are two geographically distinct groups, with the seven westernmost samples having lower Rb/Sr ratios than the three high-SiO_2 rhyolites from close to Las Plumas.

Table 4
Rb–Sr WR ages and initial $^{87}Sr/^{86}Sr$ of Jurassic volcanic rocks of Patagonia

Locality	Age (Ma)*	n**	MSWD	$(^{87}Sr/^{86}Sr)_0$	Ref.
Marifil Complex:					
Sierra Pailemán (1)	188 ± 1	9	2.9	0.7072 ± 0.0001	2
Sierra Grande (2)	174 ± 2	10	0.5	0.7127 ± 0.0006	2
Estancia Marifil (3)	183 ± 2	4	0.3	0.7068 ± 0.0001	1
Sierra Negra (4)	181 ± 7	15	0.2	0.7068 ± 0.0002	1
Dique Ameghino (5)	181 ± 4	10	10.6	0.7065 ± 0.0004	1
Río Chubut (6)	169 ± 6	10	7.9	0.7066 ± 0.0002	2
Península Camarones (7)	178 ± 1	10	1.5	0.7067 ± 0.0001	1
Chon-Aike complex (8)	168 ± 2	8	2.6	0.7066 ± 0.0001	3
Bajo Pobre formation (10)	(175)	6	-	0.7067 ± 0.0006	2

* errors are 2σ.
** n = number of samples.
All results from isochron plots except the Bajo Pobre basaltic andesites, for which an age of 175 Ma is assumed.
References: 1 = Rapela and Pankhurst [6]; 2 = this work; 3 = Pankhurst et al. [10].

Recent Ar–Ar dating has yielded comparable ages and conclusions [11].

The most striking geochemical characteristic of these rhyolitic rocks is their generally constant mean initial $^{87}Sr/^{86}Sr$ ratio of 0.7067 ± 0.0005, as noted previously by Rapela and Pankhurst [6]; this is emphasized in Table 4, which now represents data for more than 60 silicic volcanic samples. Initial $^{87}Sr/^{86}Sr$ ratios are only slightly higher (0.7072) for the majority of the samples from Sierra Pailemán and two from Sierra Grande. It was suggested above that secondary alteration might be responsible for the isochron intercept of 0.7127 for the rest of the Sierra Grande samples.

The total range of ϵNd_t for the Marifil complex is −3.9 to −8.2 (Table 2). Only the three samples from Estancia Marifil/Sierra Negra have values below −6.0; the remaining eight average −4.5 ± 0.7 (1σ). This confirms the Rb–Sr indication that the source region did not have long-term LIL-depleted characteristics. Two samples of Chon-Aike rhyolites have ϵNd_t values of −1.9 and −3.9. The analysed andesitic rocks of the Bajo Pobre Formation have initial $^{87}Sr/^{86}Sr$ ratios and ϵNd_t values indistinguishable from the majority of the rhyolites (0.7067 ± 0.0005 and −3.8 to −4.3, respectively). Moreover, the andesite–dacite rocks of Sierra Pailemán, Dique Ameghino and (with one exception) Río

Chubut show no difference in Nd and Sr isotope systematics from the accompanying rhyolitic ignimbrites, and the intermediate rocks fall on the local Rb–Sr isochrons for the acid rocks.

5. Geochemistry

Representative geochemical analyses are given in Table 3. The whole province is dominated by high-K rhyolites, with K_2O generally ranging 4–9%. SiO_2 varies 53–80%, but in most areas it is restricted to > 70%. There is a trend to quartz-normative trachydacite, sometimes defined as transalkaline [12] and dacite (Fig. 3). Because of the high SiO_2, major element plots are unable to distinguish between calc-alkaline and tholeiitic parentage, but REE patterns are typical of calc-alkaline sequences (Fig. 4), with La_N mostly > 100 and $[La/Lu]_N > 10$. Negative Eu-anomalies ($Eu/Eu^* = 0.25–0.7$) increase in magnitude with increasing SiO_2, but in the high-silica range this is accompanied by *decreasing* total REE contents, as in other orogenic calc-alkaline sequences.

Metaluminous and peraluminous compositions occur and most of these rocks would be classified as sub-alkaline [13], but in Península Camarones there is a further trend to a peralkaline sub-type with high Zr (425–600 ppm) and TiO_2 (0.45–0.95). The acidic rocks from localities 3–9 are characterized by Rb 100–250 ppm, Rb/Sr 0.2–10, $K/Rb < 170$, $Na_2O > 1.7\%$. The majority of these plot in the Volcanic

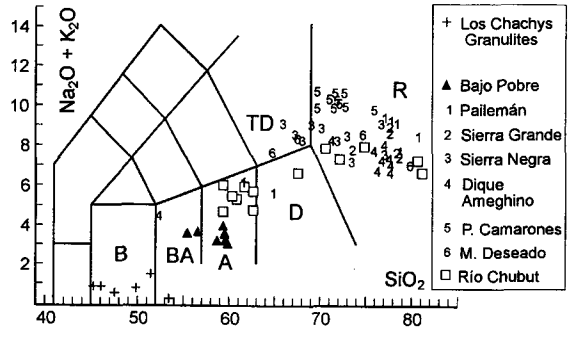

Fig. 3. Alkali–silica variation diagram. Numbers refer to localities shown in Fig. 1. Rock types: *BA* = basaltic andesite, *A* = andesite, *D* = dacite, *TD* = trachydacite, *R* = rhyolite. In the text we distinguish low-silica and high-silica rhyolites with < and > 74% SiO_2.

Arc Granite field of the Rb vs. (Y + Nb) diagram, although the peralkaline sub-type extends into the Within-Plate Granite field.

A minor highly evolved group of rhyolites is defined by samples from Sierra Pailemán and Sierra Grande in the most northerly exposures of the Marifil complex (localities 1 and 2) and also from some localities of the Chon-Aike complex. These are peraluminous, with biotite as the only mafic mineral, and typically have $SiO_2 > 75\%$, K_2O 6–9%, Rb > 350 ppm, Rb/Sr 5–35, $K/Rb < 170$, $Na_2O < 1.4\%$. The low K/Rb ratios are typical of pegmatitic–hydrothermal differentiation trends [14]. In the Rb vs. (Y + Nb) discrimination diagram these highly evolved rhyolites plot entirely within the "Syn-Collisional Granite" field, which may also be due to late-stage hydrothermal alteration. A previous geochemical study of the Chon-Aike complex indicated that its K_2O enrichment was not a primary characteristic but was acquired during post-emplacement hydrothermal alteration [15].

Less evolved rocks (55–65% SiO_2) are sometimes mappable as separate units (e.g. the medium-K andesites of the Bajo Pobre and the Lonco-Trapial formations) but also occur as a very minor phase within the rhyolite outcrops (e.g. an andesite–dacite flow at Sierra Pailemán and a basaltic andesite dyke at Dique Ameghino). These rocks have calc-alkaline major element chemistry, REE patterns with $[La/Lu]_N$ ranging 6–17 with no, or very slight, negative Eu anomalies (Fig. 5), K/Rb ratios 220–420 and Zr/Y 6–12. The slope of the REE patterns of these less evolved rocks seems to correlate with N–S variations in age: the northern (and older) locations have $[La/Lu]_N$ ratios of ca. 17, decreasing to 13 for Río Chubut and to 6–7 for the Bajo Pobre andesites. The Bajo Pobre andesites are also significantly less enriched in other lithophile trace elements than those from Río Chubut and Sierra Pailemán, which have comparable LREE-enriched patterns to the dacites and trachydacites. Although there is an overall continuity between the composition of these intermediate rocks and the dominant rhyolites of the province, at individual localities there is always a *variable* gap in SiO_2 between intermediate and acid volcanic rocks (see Fig. 3).

Fig. 4 summarizes REE patterns for the acid and intermediate volcanic rocks. In each area there are

special features, presumably due to local variations in melting and fractionation, but some general characteristics are shared by the whole province. Wherever intermediate rocks in the range 62 to 67% SiO_2 have been identified, their REE patterns show a continuous transition to those of the rhyolitic rocks, with increasingly negative Eu anomalies (accompanied by decreasing Sr content) and decreasing La/Yb ratio (localities 1, 3, 4, 5). Where high-silica rhyolites (> 77% SiO_2) occur, they display the largest Eu anomalies, with significant decrease in total REE contents, sometimes to below the levels in the intermediate volcanic rocks. This is probably due to fractionation of REE-rich accessory minerals (localities 2, 4, 6). In at least in one case (locality 2) there is also middle REE depletion.

6. Petrogenesis of the silicic volcanic rocks

The wide range of major element compositions throughout the province, as well as the evidence for eruption from southward-migrating centres over a period of perhaps 20 Ma, precludes simple co-magmatic relationships between all samples. The distinctive trace element characteristics of each centre also

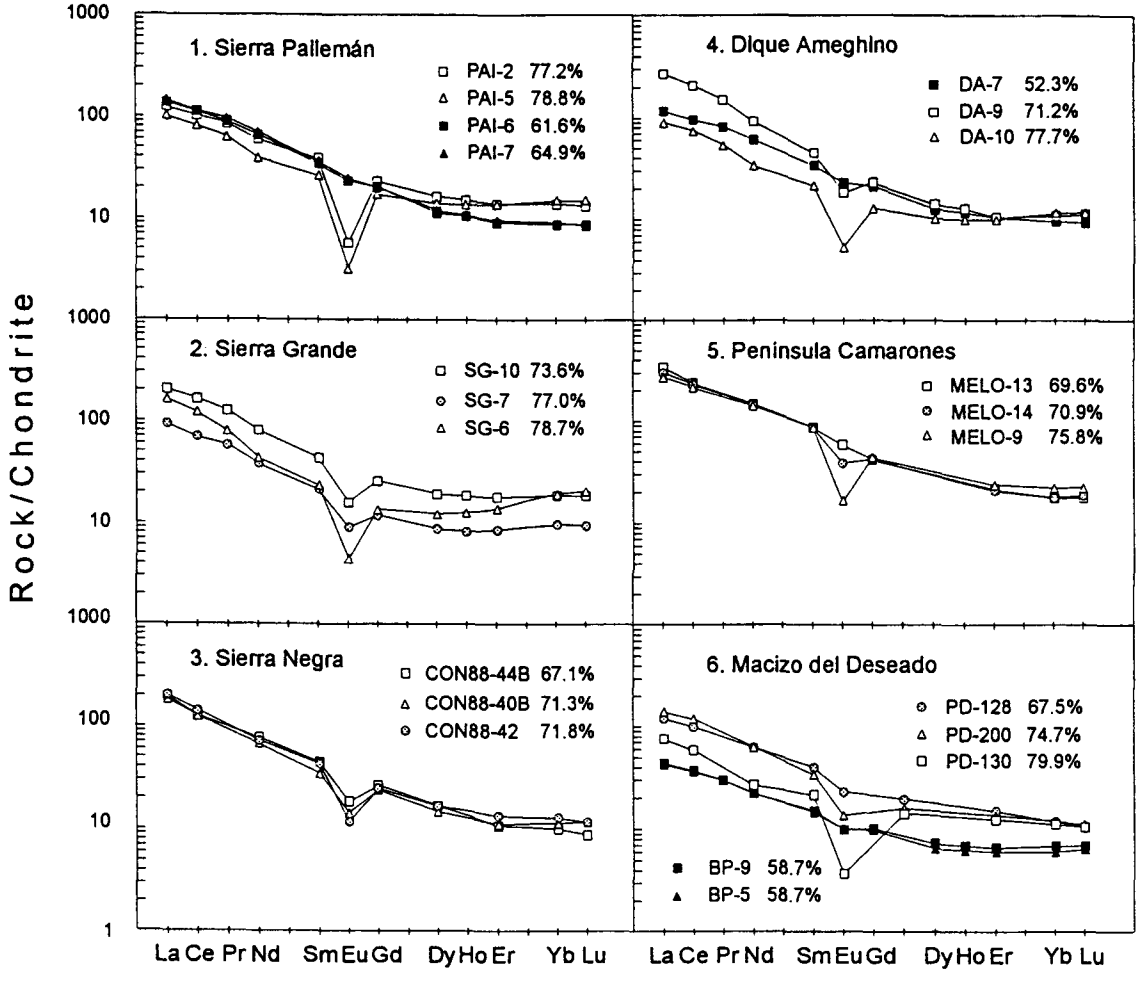

Fig. 4. Chondrite-normalized (essentially [26]) REE patterns for representative Jurassic rhyolites from each of the main centres in eastern Patagonia. Data for Macizo del Deseado silicic samples are from Sruoga [15], determined by INAA at Cornell University. The figure given after each sample number is its SiO_2 content.

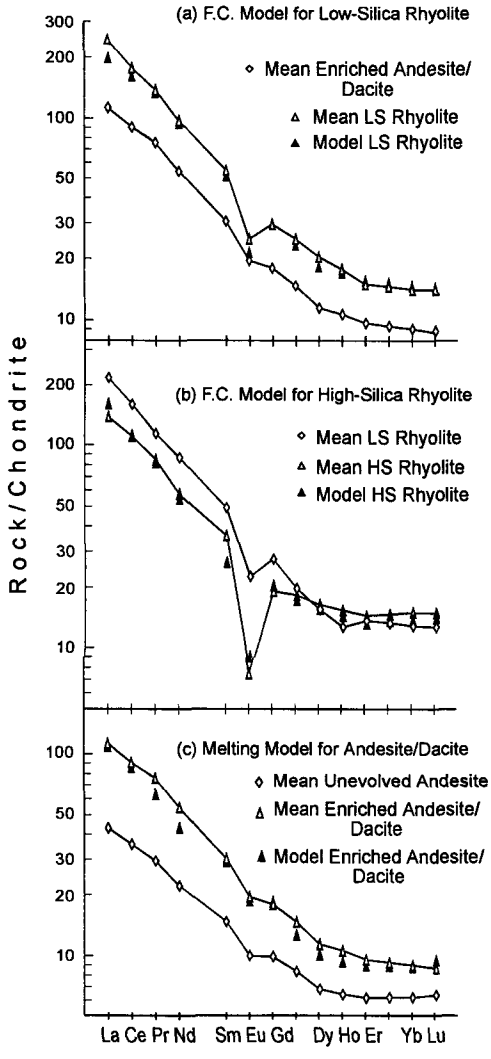

Fig. 5. Evolution of the Jurassic volcanic rocks of the Marifil and Chon-Aike groups, based on generalized REE distributions. (a) Rayleigh FC model for the production of low-silica rhyolite (mean of 11 samples) from enriched andesite/dacite (see text; mean of 6) by the removal of 50% crystal assemblage (10% amphibole, 90% plagioclase); (b) Rayleigh FC model for the production of high-silica rhyolite (mean of 11) from the mean low-silica rhyolite by the removal of 40% crystal assemblage (40% hornblende, 1% apatite, 0.05% allanite, the balance as plagioclase); (c) Batch melting of depleted Bajo Pobre basaltic andesite (mean of 3) to produce the mean andesite/dacite of Fig. 5a. Melt extraction is 20% and the residual assemblage consists of 80% orthopyroxene and 20% plagioclase. Distribution coefficients from [27], except for sanidine [28] and allanite [29] in Fig. 5b. Values interpolated for elements not determined.

require local differences in sources and differentiation processes. Nevertheless, uniform initial isotopic compositions argue for a broadly common origin and an isotopically homogeneous primary magma type that was widespread within the province.

The behaviour of REE described above and the common Nd–Sr isotopic signatures suggest some form of liquid–crystal fractionation. The sequence from dacite to low-silica rhyolite to high silica–rhyolite can be modelled by simple fractional crystallization. Fig. 5 (a and b) models successive stages of fractionation of the LIL-enriched andesites and dacites within high level magma chambers, mainly by the removal of plagioclase feldspar and amphibole (with trace amounts of accessory minerals for the high-silica rhyolites, as indicated by the falling REE contents). Rb and Sr variations are also largely explained largely by these models. Multi-stage remelting within the volcanic pile could equally explain these variations—the important point is that crystal–liquid fractionation is the fundamental process responsible. Further constraint on mechanisms through major element modelling is beyond the scope of this paper and requires more detailed (electron probe) data on the phenocryst phases.

7. Relationship between the mafic and silicic rocks.

The silicic magmas clearly did not originate within the upper crust, as proposed for the Tobífera rhyolites by Bruhn et al. [16], but it is unlikely that such large volumes of siliceous magmas were generated within the mantle. Their persistent mean initial $^{87}Sr/^{86}Sr$ ratio of 0.7067 and unradiogenic Nd isotope compositions also are unrepresentative of a normal mantle source (Table 4). Their isotopic comparability to the basaltic andesites and andesites of the region indicate co-genesis, but the large relative enrichment of LIL elements would necessitate excessive degrees of fractional crystallization in a liquid–liquid model. For example, the three-fold increase in La, Ce and Nd from the least evolved Bajo Pobre basaltic andesites to the mean andesite/dacite illustrated in Fig. 5a, would require around 70% removal of a cumulates for this stage alone. Alternatively, the silicic rocks could be partial re-melts of andesite magmas that had crystallized in the lower crust. A

simple scenario for this is illustrated in Fig. 5c, where the REE contents of the mean dacite liquid can modelled as a 20% melt of the Bajo Pobre andesites, leaving a harzburgitic residue, although this would also require that some Rb were retained in residual phlogopite.

As to the source of the unevolved andesites themselves, there are two potential source regions compatible with their isotopic and trace element characteristics: an enriched lithospheric upper mantle, as proposed for the Tobífera and its probable time-equivalents in the Antarctic Peninsula Volcanic Group [17], and a juvenile or LIL-element poor lower crust.

An argument against the presence of enriched mantle in northern Patagonia is provided by the isotopic composition of the widespread Tertiary plateau basalts of Somuncurá [18]. These rocks are thought to have been derived from both lithospheric and asthenospheric upper mantle sources, with minimum crustal contamination. Initial $^{87}Sr/^{86}Sr$ ratios mostly in the range 0.7030 to 0.7050 and ϵNd_t values -2 to $+4.5$ are quite distinct from those of the Jurassic rocks. According to Kay et al. [18], the samples with the highest proportion of lithospheric component have the lowest initial $^{87}Sr/^{86}Sr$ ratios (0.7032–0.7038).

The Nd-isotope systematics of the Jurassic volcanic rocks, both mafic and silicic, give reasonably uniform model ages for separation from depleted mantle of 1200–1500 Ma (Table 2). This is similar to the range shown by most Palaeozoic and Jurassic granitoids and metasedimentary rocks in Patagonia, interpreted as indicating lower crust formation throughout the region during Late Proterozoic times (''Grenvillian'', s.l.) [19]. If any of the Jurassic magmas were really derived from lithospheric mantle, the latter must also have been formed in this Late Proterozoic event and remained fossilised as a complementary paired system with the overlying lower crust though Phanerozoic times. A lower crustal source is our preferred option, and is developed in the following section.

8. Lower crustal xenoliths

At a number of localities within the Tertiary volcanic field of the North Patagonian Massif, there are minor ultrapotassic intrusions, genetically very distinct from the plateau basalts. One such occurrence at Sierra de Los Chacays has been dated at 19.3 ± 0.3 Ma (1σ error, [20]). The ultrapotassic rocks here contain granulitic xenoliths considered to be of lower crustal origin [7]—the only described examples of lower crustal material from the region of the Patagonian acid volcanic province. A small collection was analysed to determine their possible role in Jurassic magma generation.

The samples are large (10–40 cm) foliated nodules composed of pyroxenite (cpx + opx) or banded plagioclase–pyroxenite (opx + cpx + magnetite + spinel): petrographically they are extremely fresh. Such lithologies are unknown from basement outcrops in Patagonia. They have SiO_2 45–51%, K_2O c. 0.1%, Al_2O_3 15.7–28.0%, total FeO 4.5–12.5%, MgO 9–18%, and are highly depleted in incompatible trace elements: Rb 1–2 ppm, K/Rb 550–950, Y 2–9 ppm. Their total REE content is 9.5 to 22 ppm, with $[La/Yb]_N$ 7–12, $[La/Sm]_N$ 0.93–1.4 and variable positive Eu-anomalies (Fig. 5). $^{87}Sr/^{86}Sr$ ratios at the time of eruption range 0.70618–0.70782 (each value precise to 0.01%, 1σ), encompassing the initial $^{87}Sr/^{86}Sr$ ratio of the host latite (0.70629). Corbella and Barbieri [22] reported a comparable value of 0.70623 for the latter based on a whole-rock isochron and emphasized that the latites and the nodules were isotopically unlike the Tertiary basalts. However, we do not believe that the xenoliths were cumulates from the host magma—their isotopic compositions are too inhomogeneous for such a direct relationship (e.g. their ϵNd_t values at 30 Ma range from -1.7 to -7.4 and are only equivalent to the -3.2 of the latite on average). The differences in trace element contents are also too extreme (factors of 200, 100 and 25 for K, Rb and Nd, respectively). Six samples analysed yield $^{87}Sr/^{86}Sr$ ratios at 180 Ma of 0.70584–0.70781, with a mean of 0.70669 ± 0.00064 (1σ). Despite the variation, the mean value is remarkably close to those of both the Jurassic acid volcanic rocks and the Bajo Pobre basaltic andesites (Table 4). ϵNd_t values for the nodules at 180 Ma range from -2.2 to -6.8, but with a mean of -3.9, again indistinguishable from the means of the Marifil and Chon-Aike rhyolites and the Bajo Pobre andesites. These considerations lead us to propose a genetic link between the Jurassic magmas and these

LIL-depleted lower crustal xenoliths. Either the latter were cumulates from the primary magmas in mid-Jurassic times, or else they represent the residue of the source region after magma extraction. It is extremely difficult to distinguish these two possibilities: the "metamorphic" assemblage of pyroxene and spinel and granoblastic textures suggest that they could be restite, whereas their genrally high Mg-numbers (ca. 80) suggest a probable cumulate origin. The range of their Sr and Nd isotopic compositions calculated for 180 Ma exceeds that of the majority of the Jurassic volcanic rocks themselves, and they cannot be unaltered cumulates from a homogeneous magma.

Simple geochemical modelling constrains the relationship between the Sierra de Los Chacays nodules and the Jurassic magmas. The average mineralogical composition of the nodules was estimated from the banded xenoliths, NCHAC-1, -2, -3 and -7. Using conventional liquid–crystal partition coefficients for basaltic melts, Rb and Sr contents of a liquid in equilibrium with this assemblage were calculated as Rb = 28–56 ppm, Sr = 463–664 ppm. These compare well with the range exhibited by the Bajo Pobre andesites (Table 1), allowing for some plagioclase fractionation. Similar calculations for REE concentrations are illustrated graphically in Fig. 6. The model predicts a melt pattern with a subhorizontal HREE and LREE fractionation, similar to that of the most primitive Bajo Pobre andesites of the Jurassic province (Fig. 5c).

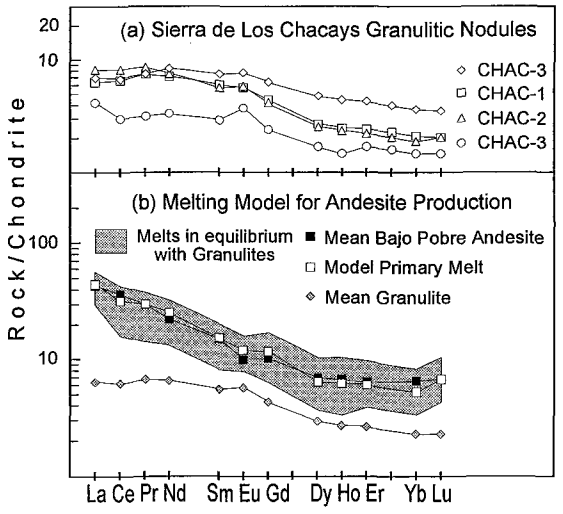

Fig. 6. (a) Chondrite-normalized REE patterns for the Sierra de Los Chacays granulitic nodules. (b) REE equilibrium melting model for generation of the depleted Bajo Pobre andesite magmas, taking the Sierra de Los Chacays nodules to represent the refractory residue: modal composition = plagioclase feldspar 44–51%, opx 11–18%, cpx 23–30%, spinel 3–5%, magnetite 1–10%. The shaded area is the field of basalt/andesite liquids in equilibrium with the analysed samples; phenocryst/matrix partition coefficients from [30]. The model is also consistent with the nodules representing cumulates from the andesitic magmas. Values interpolated where necessary.

9. Comparison with Sierra Madre Occidental

The rocks of the Marifil and Chon-Aike complexes show many similarities to the Tertiary rhyolite–ignimbrite field of the Sierra Madre Occidental (SMO), Mexico. Cameron and co-workers [1,2] studied the geochemistry and isotope geology of the SMO and concluded that geochemical variability was best explained by fractional crystallization from primary mantle-derived basalts—a theme developed extensively in subsequent publications. We have emphasised above that the crystal–liquid fractionation relationships of the Patagonian silicic rocks can equally be explained by multi-stage re-melting of a mafic source within the crust. Morover, the Patagonian rocks studied are both more uniform and more crustal in their isotopic characteristics than the SMO rocks, which have initial $^{87}Sr/^{86}Sr$ ratios 0.7045–0.707 and ϵNd_t values +6 to −2. Ruiz et al [3] concentrated on the similarity of SMO Nd isotope compositions to those of lower crustal xenoliths and exposed basement rocks, and concluded that the silicic volcanic rocks were principally derived by re-melting of Precambrian lower crust. In a more complete study of xenoliths Cameron et al. [21] distinguished several varieties. Those most similar to the Sierra de Los Chacays xenoliths are mafic granulites, which they interpreted as mid-crustal cumulates from the Tertiary magmas. However, the SMO mafic granulites have the most primitive isotope compositions of all the xenoliths (initial $^{87}Sr/^{86}Sr$ ratio 07045–0.7050 with the exception of one sample at 0.7070 which is admitted to be a pre-Cenozoic restite), and in this respect they are not comparable to the xenoliths that we have analysed.

Regardless of the relative importance of partial melting and fractional crystallization in the petrogenesis of either province, we are also impressed by the crustal Nd-isotope signatures. The Patagonian rocks (intermediate to silicic volcanic rocks and mafic granulites) have more uniformly negative ϵNd_t values, and very consistent mid-to-late Proterozoic model ages. As pointed out above, even if the primary mafic material were derived from enriched lithospheric mantle, this itself must have undergone its LIL-enrichment more than 1000 Ma ago. The SMO volcanic rocks and xenoliths also have mid-to-late Proterozoic T_{DM} model ages, and could equally be intepreted in this way. It is important to emphasize that T_{DM} ages only give an indication of the likely original age of mantle separation of lower crustal material, which might have undergone re-working in the Palaeozoic. This is a clear possibility in Patagonia, where Palaeozoic granitoids also have the same Proterozoic Nd-isotope signatures as the Jurassic volcanic rocks.

10. Conclusions and tectonic significance.

The Jurassic silicic volcanic rocks of the Marifil and Chon-Aike complexes, part of one of the largest rhyolitic provinces known, vary considerably in major and trace element composition, but were effectively uniform in their Sr and Nd isotopic compositions. Rb–Sr whole-rock dating has proved to be a very suitable technique for these rocks, and reveals that within each minor centre eruption occurred over a short interval (within 1–2 Ma in most cases) but that overall activity persisted over some 20 Ma, with apparent migration towards the south.

The isotopic uniformity, supported by simple REE modelling, shows that internal variability was controlled by crystal–liquid fractionation. In general this does not distinguish fractional crystallization from variable partial melting and it is likely that both mechanisms were involved. We have modelled the production of LIL-enriched andesites and dacites by the partial melting of more a more LIL-depleted basaltic andesite or andesite, represented by the Bajo Pobre Formation of the Deseado Massif. On the other hand, evolution within each centre from dacite to high-silica rhyolite has been modelled mainly as a fractional crystallization process. Neither of these models is exclusive, but the overall cogenetic nature of the magmas is established.

All the magmas, both the predominant silicic ones and the most mafic ones observed (basaltic andesite), had initial isotopic compositions unlike the mantle-derived Tertiary basalts of Patagonia. The isotopic data are consistent with a Late Proterozoic (''Grenvillian'') lower crustal source, albeit it a low Rb/Sr mafic one. Simple mass-balance suggests extraction of about 30% melt for formation of the primary andesite. Even if the xenoliths were cumulates from the primary MACHO andesites, a chemically and isotopically comparable source would still be indicated. In principle then, we agree with Ruiz et al. [3], that such rhyolitic large igneous provinces represent re-working of previously differentiated (and probably crustal) sources, rather than extensive primary crust-formation.

The heat source for crustal anatexis is problematical, unless produced by unrelated but contemporaneous mantle-derived basalt magmatism. There is no direct evidence for Jurassic mantle-derived magmatism in Patagonia itself, but in adjacent parts of Gondwana this was the time at which the extremely voluminous Ferrar dolerites and related mafic rocks were formed. We believe that extensive lower crustal melting was related to the tectonic environment associated with the rifting and incipient break-up of the Gondwana supercontinent [22]. Evidence from experimental petrology [23] has shown that fluid-absent partial melting of amphibolite at about 30 km depth can reach unexpectedly large degrees at relatively low temperatures (e.g. 20% at ca. 850°C) and may be triggered by crustal thinning processes without too much additional heat input. Rifting was well underway by mid-Jurassic times, and involved large-scale migration of the southern Patagonian region away from the shield areas coring the landmass [24,25]. The contemporaneity of these movements, combined with extension and thinning of the crust and the simultaneous emplacement of the ''Ferrar'' suite of mafic magmas may have provided the unique set of conditions that produced this rhyolitic ''flare-up''. There is no obvious need to relate this event either to subduction or to a mantle plume.

Acknowledgements

Financial support for fieldwork from CONICET, Argentina (Grants PID-BID 0123 and PID 3661/92) and the Royal Society, London is acknowledged. M. Haller introduced us to the Marifil complex and P. Sruoga provided samples and data for Chon-Aike rocks. A.J. Wlasiuk, C. Cavarozzi, V. Posadas gave technical assistance in Argentina, and A. Robertson and M. Ingham (British Geological Survey) in Keyworth. The manuscript benefitted from the comments of P.D. Kempton, P.T. Leat, S.M. Kay, R.L. Rudnick and J. Ruiz. This paper is recorded as NIGL Publication No. 130 and is a contribution to IGCP Project No. 345 "Andean Lithospheric Evolution".

References

[1] M. Cameron, W.C. Bagby and K.L. Cameron, Petrogenesis of voluminous mid-Tertiary ignimbrites of the Sierra Madre Occidental, Contrib. Mineral. Petrol. 74, 271–284, 1980.

[2] K.L. Cameron and M. Cameron, Rare earth element $^{87}Sr/^{86}Sr$ and $^{143}Nd/^{144}Nd$ compositions of Cenozoic orogenic dacites from Baja California, northwestern Mexico and adjacent west Texas: evidence for the predominance of a subcrustal component, Contrib. Mineral. Petrol. 91, 1–11, 1985.

[3] J. Ruiz, P.J. Patchett and R.J. Arculus, Nd–Sr isotope composition of lower crustal xenoliths—evidence for the origin of mid-Tertiary felsic volcanics in Mexico, Contrib. Mineral. Petrol. 99, 36–43, 1988.

[4] D.A. Gust, K.T. Biddle, D.W. Phelps and M.A. Uliana, Associated Middle to Late Jurassic volcanism and extension in southern South America, Tectonophysics 116, 223–253, 1985.

[5] S.M. Kay, V.A. Ramos, C. Mpodozis and P. Sruoga, Late Paleozoic to Jurassic silicic magmatism at the Gondwana margin; analogy to the Middle Proterozoic in North America? Geology 17, 324–328, 1989.

[6] C.W. Rapela and R.J. Pankhurst, El volcanismo ríolitico del noreste de la Patagonia: un evento meso-jurásico de corta duración y origen profundo, Actas del XII Congreso Geológico Argentino, Mendoza (10–15 October 1993), Alcira Vergara Oroño, Buenos Aires, IV, 179–188, 1993.

[7] H. Corbella, Hallazgo de rocas leucíticas, perpotásicas en la Sierra de los Chacays, Patagonia extrandina, Provincia de Chubut. Rev. Assoc. Argentina Mineral. Petrol. Sedimentol. 14, 88–96, 1983.

[8] C. Miniussi, J.C. Merodio, V.G. Posadas and J. Meda, Determinación de elementos minoritarios y traza por fluorescencia de rayos-X, Rev. Assoc. Argentina Mineral. Petrol. Sedimentol. 11, 15–21, 1980.

[9] J.M. Cortés, El substrato precretácico del extremo noreste de la Provincia del Chubut, Rev. Assoc. Geol. Argentina 36, 211–235, 1981.

[10] R.J. Pankhurst, P. Sruoga and C.W. Rapela, Estudio geocronológico Rb–Sr de los complejos Chon-Aike y El Quemado a los 47°30′ L.S. Actas XII Cong. Geol. Argentino, Mendoza (10–15 October 1993), Alcira Vergara Oroño, Buenos Aires, IV, 171–178, 1993.

[11] V. Alric, G. Feraud, H. Bertrand, M. Haller, C. Labudia and M. Zubia, $^{40}Ar/^{39}Ar$ dating of Patagonian Jurassic volcanism: new constraints on Gondwana break-up, Terra Nova 7, Abstract Suppl. 1, 353, 1995.

[12] E.A.K. Middlemost, Towards a comprehensive classification of igneous rocks and magmas, Earth-Sci. Rev. 31, 73–87, 1991.

[13] A. Myashiro, Nature of alkalic volcanic rock series, Contrib. Mineral. Petrol. 66, 91–104, 1978.

[14] D.M. Shaw, A review of K–Rb fractionation trends by covariance analysis, Geochim. Cosmochim. Acta 32, 573–601, 1968.

[15] P. Sruoga, Estudio petrológico del Plateau ignimbrítico jurásico a los 47°30′ lat.S. Ph.D. thesis, Univ. Nacional La Plata, Argentina (unpubl.), 1989.

[16] R.L. Bruhn, C.R. Stern and M.J. De Wit, Field and geochemical data bearing on the development of a Mesozoic volcano–tectonic rift zone and back-arc basin in southernmost South America, Earth Planet. Sci. Lett. 41, 32–46, 1978.

[17] B.C. Storey and T. Alabaster, Tectonomagmatic controls on Gondwana break-up models: evidence from the proto-pacific margin of Antarctica, Tectonics 10, 1274–1288, 1991.

[18] S.M. Kay, A.A. Ardolino, M. Franchi and V.A. Ramos, El origen de la meseta de Somún Curá: distribución y geoquímica de sus rocas volcanicas máficas, Actas XII Cong. Geol. Argentino, Mendoza (10–15 October 1993), Alcira Vergara Oroño, Buenos Aires, IV, 236–248, 1993.

[19] R.J. Pankhurst, F. Hervé and C.W. Rapela, Sm–Nd evidence for the Grenvillian provenance of the metasedimentary basement of Southern Chile and West Antarctica. Actas VII Cong. Geol. Chileno, Concepción, II, 1414–1418, 1994.

[20] H. Corbella and M. Barbieri, Sierra de los Chacays, Patagonia extrandina, Provincia de Chubut: $^{87}Sr/^{86}Sr$ isotopic ratios of the alkaline rocks and age of the potassic volcanics of Mt. Platt Luan, Rev. Assoc. Geol. Argentina 44, 133–140, 1989.

[21] K.L. Cameron, J.V. Robinson, S. Niemeyer, G.J. Nimz, D.C. Kuentz, R.S. Harmon, S.R. Bohlen and K.D. Collerson, Contrasting styles of mid-Tertiary crustal evolution in northern Mexico: evidence from deep crustal xenoliths from La Olivina, J. Geophys. Res. 97B, 17353–17376, 1992.

[22] B.C. Storey, T. Alabaster, M.J. Hole, R.J. Pankhurst and H.E. Wever, Role of subduction plate boundary forces during the initial stages of Gondwana break-up: evidence from the proto-Pacific margin of Antarctica, in: Magmatism and the Causes of Continental Break-up, B.C. Storey, T. Alabaster and R.J. Pankhurst, eds., Spec. Publ. Geol. Soc. London 68, 149–163, 1992.

[23] T. Rushmer, Partial melting of two amphibolites: contrasting experimental results under fluid-absent conditions, Contrib. Mineral. Petrol. 107, 41–59, 1991.

[24] C.W. Rapela and R.J. Pankhurst, The granites of northern Patagonia and the Gastre Fault System in relation to the break-up of Gondwana, in: Magmatism and the Causes of Continental Break-up, B.C. Storey, T. Alabaster and R.J. Pankhurst, eds., Spec. Publ. Geol. Soc. London 68, 209–220, 1992.

[25] Z. Ben-Avraham, C.J.H. Hartnady and J.A. Malan, Early tectonic extension between the Agulhas Bank and the Falkland Plateau due to the rotation of the Lafonia microplate, Earth Planet. Sci. Lett. 117, 43–58, 1993.

[26] N. Nakamura, Determination of REE, Ba, Fe, Mg, Na and K in carbonaceous and ordinary chondrites, Geochim. Cosmochim. Acta, 38, 757–773, 1974.

[27] C.R. Bacon and T.H. Druitt, Compositional evolution of the zoned calcalkaline magma chamber of Mount Mazama, Crater Lake, Oregon, Contrib. Mineral. Petrol. 98, 224–256, 1988.

[28] W.P. Nash and H.R. Crecraft, Partition coefficients for trace elements in silicic magmas, Geochim. Cosmochim. Acta 49, 2309–2322, 1985.

[29] G. Mahood and W. Hildreth, Large partition coefficients for trace elements in high-silica rhyolites, Geochim. Cosmochim. Acta 47, 11–30, 1983.

[30] P. Henderson, General geochemical properties and abundances of the rare earth elements, in P. Henderson, ed., Rare Earth Element Geochemistry, Elsevier, Amsterdam, pp. 1–32, 1984.

[31] D.J. DePaolo, A.M. Linn and G. Schubert, The continental crustal age distribution: methods of determining mantle separation ages from Sm–Nd isotopic data and application to the Southwestern United States, J. Geophys. Res. 96B, 2071–2088, 1991.